Development of an amplicon-based high throughput sequencing method for genotypic characterisation of norovirus in oysters

Amy H Fitzpatrick[1,2,3], Agnieszka Rupnik[2], Helen O'Shea[3], Fiona Crispie[1], Paul D. Cotter[1], Sinéad Keaveney*[2]

[1] Department of Food Biosciences, Teagasc Food Research Centre, Fermoy, Ireland

[2] Department of Shellfish Microbiology, Marine Institute, Oranmore, Ireland

[3] Department of Biological Sciences, Munster Technological University, Cork, Ireland

*Corresponding author: sinead.keaveney@marine.ie

Keywords: environmental virology, Caliciviridae, Illumina, DNA polymerase, reverse transcriptase

Abstract

Norovirus is a highly diverse RNA virus often implicated in food-borne outbreaks, particularly shellfish. Shellfish are filter feeders, and when harvested in bays exposed to wastewater overflow or storm overflows, they can harbour various pathogens, including human pathogenic viruses. The application of Sanger or amplicon-based High Throughput Sequencing (HTS) technologies to identify human pathogens in shellfish faces two main challenges i) distinguishing multiple genotypes/variants in a single sample and ii) low concentrations of norovirus RNA.

Here we have assessed the performance of a novel norovirus capsid amplicon HTS method. We generated a panel of spiked oysters containing various norovirus concentrations with different genotypic compositions. Several DNA polymerase and Reverse Transcriptase (RT) enzymes were compared, and performance was evaluated based on i) the number of reads passing quality filters per sample, ii) the number of correct genotypes identified, and iii) the sequence identity of outputs compared to Sanger-derived sequences. A combination of the reverse transcriptase LunaScript and the DNA polymerase AmpliTaq Gold provided the best results. The method was then employed, and compared with Sanger sequencing, to characterise norovirus populations in naturally contaminated oysters.

Importance

While foodborne outbreaks account for approximately 14% of norovirus cases (Verhoef L, Hewitt J, Barclay L, Ahmed S, Lake R, Hall AJ, Lopman B, Kroneman A, Vennema H, Vinjé J, Koopmans M. 2015. 1999-2012. Emerg Infect Dis 21:592–599),

we do not have standardised high-throughput sequencing methods for genotypic characterisation in foodstuffs. Here we present an optimised amplicon high-throughput sequencing method for the genotypic characterisation of norovirus in oysters. This method can accurately detect and characterise norovirus at concentrations typically detected in oysters. It will permit the investigation of norovirus genetic diversity in complex matrices and contribute to ongoing surveillance of norovirus in the environment.

Introduction

In norovirus outbreaks associated with the consumption of shellfish, clinical and shellfish samples collected during the outbreak investigation are often subjected to nucleic acid Sanger sequencing for source attribution. The application of Sanger sequencing in this scenario is cumbersome in shellfish due to the need for the cloning of PCR isolates to capture the genetic diversity in a single sample (1–3) and generally only allows for low throughput analysis. High-throughput sequencing (HTS) permits low-cost sequencing, outputs high-throughput data and captures considerable nucleotide diversity, as demonstrated with 16S rRNA amplicon-based HTS analysis of bacteriomes. In contrast to Sanger sequencing, HTS technologies can also resolve multiple sequences per amplicon without cloning isolates in environmental samples.

A few studies have applied HTS-based methods for the detection and characterisation of norovirus in complex matrices such as food or wastewater (4–16). Notwithstanding these studies, the performance of the various methods, whether it be shotgun metagenomics, capture probe hybridisation, long-read

sequencing or amplicon-based HTS, has varied. While shotgun metagenomics permits a less biased approach to sequencing, sequencing depth is often insufficient to characterise the norovirus present due to the presence of nucleic acid from other sources, even after rRNA removal or polyA tail enrichment (7, 8, 11, 12, 14). Capture probe hybridisation can enrich viral sequences, which could be helpful in challenging matrices. However, current market options are expensive and do not necessarily enrich the regions used for dual-genotyping norovirus, as panels are designed to broadly target viruses rather than specific viral families (7–9, 17). Long-read sequencing methods, such as those provided by PacBio and Oxford Nanopore Technologies (ONT), also face challenges in obtaining sufficient sequencing depth in complex matrices. Indeed, their outputs are typically lower than those from short-read platforms. ONT combined with adaptive sampling has had limited success in food samples (7), while, to date, long-read ONT sequencing of norovirus amplicons has not been successful (17). Despite these challenges, several recent studies have demonstrated the capability of various amplicon HTS assays for the genotypic characterisation of norovirus in shellfish (5, 17), with similar success observed in berry samples (6). However, these studies focused on application rather than optimisation and did not confirm HTS results with the gold standard Sanger methods. Due to the high degree of underreporting of norovirus cases, particularly non-nosocomial cases in healthy populations (18, 19), samples tend to come from food-borne outbreaks requiring source attribution or chronic nosocomial cases. This skews our understanding of norovirus genotypes circulating in local populations and will limit effective vaccine production in the future and management of clinical cases (20). Considering the necessity of capturing the norovirus sequences that permit

genotypic characterisation in complex samples with low concentrations of viral RNA, this study has focused on optimising amplicon-based HTS methods.

Despite its potential value, amplicon HTS can introduce bias at multiple steps in the process, most notably RNA extraction and amplification of the target DNA. Bias during PCR cycling is impacted by choice of primers in that they are designed to target a conserved area of a chosen genome (21, 22). Currently, norovirus taxonomic assignment relies on dual genotyping based on the RNA-dependent RNA polymerase RdRp and VP1 gene (23). However, historically genotypic characterisation has focused on the VP1, also known as the capsid (24, 25). As a single-stranded RNA (ssRNA) virus, norovirus has a high mutation rate, estimated to be $5.40x10^{-3}$–$2.23x10^{-4}$ nt substitutions/site/year for the VP1 encoding region (26). For example, SARS-CoV-2 has estimated $8.066x10^{-4}$ nt substitutions/site/year for the S gene (27). Moreover, noroviruses are genetically diverse, with a relatively low shared nucleotide identity of approximately 63% across commonly sequenced regions such as region C and the breakpoint of the RdRp-VP1 (23). Thus, designing suitable primers to capture norovirus's existing and potential diversity is challenging. Various primers have been used for molecular characterisation, with most reference laboratories targeting the most conserved region of the genome (ORF1-ORF2 junction) and using degenerate primers that can tolerate sequence mismatches (25, 28). The regions typically targeted for molecular characterisation result in amplicons ranging from 113 bp to 587 bp in length (29). This study generated amplicons using primers targeting Region C (Figure 5), which yielded a 340 bp amplicon suitable for 300 bp paired-end sequencing. These primers are highly degenerate and can capture a broad range of norovirus genotypes.

110 The objective of this study was to establish a capsid amplicon-based HTS
111 method for norovirus genotyping in shellfish. Critical criteria for a successful
112 assay were as follows: i) accurate characterisation of genotypes in samples with
113 concentrations of norovirus RNA typically observed in outbreaks and ii) accurate
114 characterisation of multiple genotypes, and iii) superior performance to Sanger
115 sequencing for application in surveillance-based studies. Reverse transcription
116 (RT) and DNA polymerase enzymes are known to impact HTS outputs from
117 quality to classification accuracy (30–33), therefore, selected enzyme
118 combinations were compared in spiked and naturally contaminated samples.

119 The optimised amplicon-based HTS method and traditional Sanger sequencing
120 method were successfully applied to a panel of naturally contaminated oysters,
121 with a strong agreement between conventional and novel techniques.

122

Results

The method was optimised with clinical samples and oysters either spiked with clinical material or naturally contaminated samples. By sequencing previously characterised clinical and spiked samples, method performance could be assessed in terms of its sensitivity and specificity.

Characterisation of clinical positive control samples

To facilitate the subsequent assessment of the accuracy of HTS-based approaches, it was necessary first to source clinical samples containing specific norovirus genotypes. RT-qPCR and Sanger sequencing were used to characterise these clinical samples (Table 1), which were positive for one genotype per sample and contained a high concentration of norovirus RNA. These samples were subsequently used to spike oyster samples.

Impact of enzyme combinations on genotype detection by HTS

Three reverse transcriptase and DNA polymerase enzyme combinations were applied to clinical and spiked shellfish samples. Table 2 provides the genotypes detected in the various sequencing experiments (1-3) by the enzyme combinations. Samples in experiment one included the clinical samples (Table 1) and spiked shellfish samples that were prepared using material from the clinical samples at various concentrations and combinations (Table 9). An additional spiked shellfish sample was sourced for a comprehensive RT and DNA polymerase comparison in experiment 2. The optimised method was applied to a panel of naturally contaminated samples in experiment 3, using LunaScript with AmpliTaq Gold.

Enzyme combination impacts the quality of high throughput sequencing reads.

Selected reverse transcriptase enzymes (RT) and DNA polymerases were compared to understand if method optimisation could improve the quality of sequences obtained. Moloney murine leukaemia virus (MMLV) derived RT SuperScript II, and SuperScript IV were evaluated alongside an *in-silico* designed RT LunaScript. The polymerases were selected because AmpliTaq Gold is widely used for RNA virus sequencing; Kapa HiFi has a low error rate and is recommended for use within 16S amplicon HTS protocols on Illumina platforms. In contrast, KAPA2G Robust has a greater tolerance for PCR inhibitors and is recommended for use with challenging samples.

Results were compared based on Phred quality scores, used to indicate the measure of base quality in DNA sequencing and expected errors, which are the sum of error probabilities over the length of the read. As per Figure 1. A, mean Phred scores obtained (spiked shellfish) were significantly different when assessed using a Kruskal-Wallis test (p-value 2.96^{-12}, chi-squared = 425.56). RT and DNA polymerases are arranged from highest to lowest median Phred score, with LunaScript AmpliTaq Gold generating sequences with the highest Phred scores and LunaScript Kapa HiFi generating sequences with the lowest Phred scores. In Figure 1. B, expected errors (EE) were significantly different using a Kruskal-Wallis (p-value $< 2.2^{-16}$, chi-squared = 1971.1). LunaScript AmpliTaq Gold generated sequences with the lowest mean EE, while Luna Kapa Robust generated sequences with the highest mean EE.

A Factor Analysis of Mixed Data (FAMD) was performed to determine if RT or DNA polymerase enzyme contributed to the differences in performance in terms of quality (Figure 1). A FAMD works as a principal components analysis (PCA) for quantitative variables and a multiple correspondence analysis (MCA) for qualitative variables, allowing us to understand the relationship between numeric outcomes such as Phred score and factors such as DNA polymerase enzymes. In Figure 2. A, DNA polymerase enzymes contributed to 53% and 54% of the variation observed in dimensions 1 and 2, respectively; however, the overall cos2 value was low <0.3. A low cos2 indicates that the principal component does not perfectly represent DNA polymerase enzymes, i.e., other factors contribute to the variance observed. RT enzymes explained 22% and 49% of the variation observed in dimensions 1 and 2, respectively, though the cos2 value was low <0.3.

In summary, DNA polymerase contributed to observed differences in Mean Phred score to a greater extent than the RT enzyme. On the other hand, as presented in Figure 2. B, DNA polymerase returned 42% and 35%, while RT enzyme returned 39% and 68% for dimensions 1 and 2, respectively. Cos2 values for both reagents were low, <0.3. Accordingly, mean EE was influenced by RT more than DNA polymerase enzymes. Therefore, RT enzyme choice has a greater impact on expected mean errors, while DNA polymerase has a greater effect on mean Phred scores.

DNA polymerase impacts the relationship between input genomic material, and the number of HTS reads obtained

A Kendall rank correlation coefficient was used to compare the agreement between the concentration of DNA following library preparation or the gc/g of norovirus as determined by RT-qPCR before the semi-nested PCR to the HTS reads passing quality control. There was a perfect agreement (>0.8) between the concentration of DNA following library preparation as quantified by fluorometric measures and the resulting reads passing quality control for SuperScript II AmpliTaq Gold shellfish samples spiked with a single norovirus genotype (Table 3) (34). These correlations were not statistically significant, likely owing to the small sample size. Oyster samples that were spiked with multiple genotypes and prepared with SuperScript II AmpliTaq Gold provided a perfect agreement (>0.8) between the concentration of DNA following library preparation as quantified by fluorometric measures and the resulting reads passing quality control at statistically significant levels (Table 3). Overall, there was a weaker agreement between gc/g of norovirus as determined by RT-qPCR with reads passing quality control.

Ultimately, in naturally contaminated samples (n=9), there was a moderate non-significant agreement of 0.481 (p-value 0.10) and 0.389 (p-value 0.18), respectively, between the gc/g of norovirus as determined by RT-qPCR and concentration of DNA following library preparation as quantified by fluorometric measures and the resulting reads passing quality control.

Enzyme combination and technical triplicates can improve classification accuracy.

A confusion matrix was used to investigate further the differences in performance between reverse transcription and DNA polymerase enzymes. As can be seen in Table 4, all enzyme combinations performed well when used with spiked shellfish samples. When the mock communities were prepared individually, all enzyme combinations returned perfect scores, apart from instances where SuperScript II was applied in combination with Kapa HiFi. For this library, GII.3 was not detected in mock community 8, present at 700 gc/g (single genotype). Libraries, where a spiked sample was prepared in triplicate from semi-nested PCR with LunaScript or SuperScript IV, provided perfect f-scores, in contrast to samples prepared with SuperScript II that did not provide perfect f-scores. The spiked sample contained GI.3, GI.7 and GII.6. GI.7 was not detected in samples prepared with SuperScript II in combination with AmpliTaq Gold or Kapa Robust. When the PCR products for norovirus GI and GII were combined, a loss in sensitivity was observed, i.e., GI.3 or GI.7 were not detected (Table 5). Similar trends were observed using the Jaccard index; see Supplementary, Figure 1.

Phylogenetic distance between expected and observed sequences was affected by DNA polymerase enzyme

UniFrac is a distance matrix that measures the phylogenetic distance between sets of taxa in a phylogenetic tree. The distance is defined as the fraction of the branch length of the tree that leads to descendants from either one environment or the other, but not both. Unweighted UniFrac methods were used to compare the phylogenetic distance between sequences generated by SuperScript II RT and one of the following DNA polymerases; AmpliTaq Gold, Kapa Robust and Kapa HiFi. It demonstrated that DNA polymerase and RT enzyme explained some variations in sequencing results. DNA polymerase enzymes contributed to 35% of the variation observed in spiked shellfish. A Pairwise PERMANOVA was performed and returned significant p-values <0.05. Spiked samples prepared with SuperScript II, SuperScript IV or LunaScript RT enzymes and AmpliTaq Gold DNA polymerase returned p-values of 0.83-0.92, indicating a high similarity between obtained and expected sequences, see Supplementary Figure 2.

RT enzymes contributed to 37% of the variation observed in spiked shellfish. A post hoc test on the UniFrac distance matrix was performed using Pairwise PERMANOVA with 999 permutations and returned adjusted p-values of 0.84-0.93, respectively. This indicated high similarity between expected and obtained sequences when prepared with the same DNA polymerase, see Supplementary Figure 3.

Custom BLASTn databases were used to assess the ability of the various protocols to return a 99% match to the previously obtained Sanger sequences. SuperScript II AmpliTaq Gold and SuperScript II Kapa Robust returned a 99% BLASTn match with bit-scores >500 and e-values < 0.001 for all expected genotypes. SuperScript II Kapa HiFi I failed to produce a 99% match for the GI.9 genotype; see Supplementary Table 1.

Overall, LunaScript and AmpliTaq Gold provided the most accurate, high-quality results based on quality metrics, classification accuracy and phylogenetic distance.

HTS amplicon sequencing of the capsid region permitted the detection of additional genotypes from naturally contaminated shellfish samples compared to the conventional Sanger sequencing

Based on the preceding results, a library with naturally contaminated oysters was prepared using LunaScript in combination with AmpliTaq Gold for RT and the semi-nested PCR. Three naturally contaminated samples with varying concentrations of norovirus GII (see Table 6) were lysed and extracted for amplicon-based HTS and Sanger sequencing.

Sequences obtained using Sanger sequencing could not be genotyped using NoroNet. However, CaliciNet and the internal classifier provided strong concordance of genotype assignment with the MiSeq results, see Table 7. Technical triplicates introduced from the first round of RT-PCR provided strong agreement regarding the relative abundance observed for each genotype detected, see Supplementary Figure 4. More genotypes were detected using the amplicon HTS method than conventional Sanger sequencing of cloned variants. Three genotypes were detected using Sanger sequencing in MIC16714 (GII.6, GII.4 Sydney, GII.13), while an additional GII.7 was detected using amplicon HTS. In MIC15592, GII.14 was detected using Sanger sequencing, while amplicon HTS detected both GII.14 and GII.6.

Discussion

In this study, we have demonstrated that Reverse Transcription and DNA polymerase enzymes impact HTS library quality. RT-qPCR data on norovirus genome copies/g was a moderate indicator of obtained HTS reads. The optimised extraction and semi-nested PCR method permitted the accurate detection of norovirus in naturally contaminated oysters when combined with a custom bioinformatic pipeline. This is an essential development for environmental virology. The application of HTS to genotype norovirus in contaminated foods has been constrained due to a lack of available methods.

This study focused on reverse transcription and semi-nested PCR steps for optimisation. In terms of the quality of the sequences observed, as measured by Phred score and expected errors, combined enzyme choice shaped score profiles (Figures 1 and 2). It has been well documented that the priming strategy and the RT enzyme can impact the reverse transcription (RT) of RNA to cDNA. However, previous norovirus HTS studies using custom hexamers reported no improvement in performance compared to random hexamers (8). While RT aims to produce cDNA that faithfully reflects the starting RNA sample, several studies indicate that the RT reaction can introduce large variability (35–37).

DNA polymerase contributed more to the variation observed for mean Phred scores, while RT enzymes contributed more to the variability observed for mean expected errors (Figure 2). In particular, Kapa HiFi and KAPA Robust had higher expected errors when combined with LunaScript (Figure 2. B); conversely, AmpliTaq Gold and

LunaScript provided the lowest expected errors overall. This implies that RT and DNA polymerase combinations operate synergistically. Nonetheless, the literature on the mechanism behind varying RT and DNA polymerase enzyme performance is limited. The initial publication describing AmpliTaq Gold outlined its superior performance in complex sample types with low genomic input and/or multiple PCR assays (38). At the same time, KAPA Robust has been recommended for amplification in samples with high levels of inhibitors (39). AmpliTaq Gold has been widely applied in molecular virology (40–42), though there is limited literature evaluating its performance relative to other DNA polymerases. In this case, LunaScript combined with AmpliTaq Gold provided the highest quality sequences; however, previous studies in other complex sample types provide conflicting results (30, 32, 43–46). Several factors may contribute to the performance of RT and DNA polymerase enzymes, such as low input genomic material, RNA quality, matrix-specific factors, target-specific factors and DNA synthesis speed. PCR is a stochastic amplification process challenged by multiple templates, secondary structures and GC content (33, 47). The predicted hairpin structures in norovirus (48, 49) and the presence of multiple genotypes in shellfish challenge the development of any HTS applications. This warrants further study, as it is important to understand why performance variation is observed to optimise it.

Of note, AmpliTaq Gold provided high-quality sequences and optimal results in terms of classification accuracy when combined with specific RT enzymes, even though the semi-nested PCR assay with AmpliTaq Gold was performed with the highest number of total cycles. The number of PCR cycles is known to influence results. While a higher number of PCR cycles might increase the likelihood that rare

342 molecules are observed, it can also skew abundance estimates by amplifying the
343 biases (32, 50). However, this was not the case in this study. There are no
344 comparison studies on LunaScript, as it has only recently been added to the market,
345 but it is widely used for the RT step in the ARTIC SARS-COV-2 protocol (51).
346 AmpliTaq Gold has a slower DNA synthesis rate than the other studied polymerases;
347 Kapa HiFi and Kapa Robust. Furthermore, nanopore systems have demonstrated
348 that slower translocation rates result in high accuracy (52); therefore, faster
349 synthesis is not necessarily equally as accurate, especially in the case of highly
350 diverse amplicons.
351
352 Various attempts have been made to optimise the workflow in terms of the wet-lab
353 methodology developed. Notably, applying the ISO 15216:2017 method in
354 combination with the optimised semi-nested PCR did not successfully amplify
355 norovirus in naturally contaminated samples. Several modifications were required,
356 including the concentration of the viral RNA by eluting it into a lower volume and
357 increasing the input cDNA in the first round of the semi-nested PCR. This
358 emphasises the importance of performing method development with the target
359 matrix, i.e., in this case, naturally contaminated shellfish, as spiked shellfish samples
360 performed well without modifications. In addition, the inclusion of technical triplicates
361 incorporated in the various experiments resulted in improved results relative to
362 instances where individual samples were used. This observation is consistent with
363 previous work (17).
364
365 Furthermore, it was notable that the pooling of amplicons from norovirus GI and GII
366 PCR assays before library preparation resulted in lower classification accuracy, with

markedly fewer reads aligning to norovirus GI. While these steps increase the workload per biological sample, we find they are necessary for optimal HTS results. Enzyme choice (RT/DNA polymerase) did impact the accuracy of HTS of norovirus VP1 amplicons. Almost all combinations of enzymes returned perfect f-scores (1.00) when performed in triplicate apart from those treated with SuperScript II. Thus all genotypes known to be present in the samples were detected with no false positives. In the first experiment, clinical samples and spiked shellfish were sequenced; the presence of GI.9 was not detected using SuperScript II in combination with Kapa HiFi in a clinical sample. Indeed, the GI.9 sequence in question has four known nucleotide mismatches with the primers used in this study. No genotypes were missed using the LunaScript / AmpliTaq Gold enzyme combination in spiked samples. The high concordance between MiSeq amplicon HTS and conventional Sanger sequencing results supports method application in naturally contaminated shellfish.

An important consideration in choosing suitable samples to process using the outlined methodology is the detected norovirus gc/g as per ISO 15216:2017 (53). As per the moderate correlation between input gc/g and obtained HTS reads, we advise selecting samples greater than 100 gc/g for norovirus amplicon HTS (Table 6). Notwithstanding this recommendation, it has been observed in this study that some samples with a high concentration of viral RNA may fail to produce peaks of the expected size (2100 Bioanalyzer), while samples containing <300 gc/g may produce high-quality sequences. This is likely due to the quality and fragmentation of the norovirus RNA present in the shellfish at hand.

392 The semi-nested PCR targets the VP1 capsid region of norovirus, and the RT-qPCR
393 targets a smaller overlapping region in the VP1. Amplification or sequencing of the
394 full-length VP1 region has been used as a proxy for infectivity due to the hypothesis
395 that an intact capsid infers an intact virus capable of initiating an infection (54–57).
396 As observed in this study, spiked samples may behave differently from naturally
397 contaminated oysters as the norovirus RNA is intact. In contrast, norovirus
398 accumulated in shellfish could be degraded and fragmented by wastewater
399 treatment processes (2, 58) and/or exposure to UV in the marine environment (59,
400 60). This supported the variation in the correlation between input material and
401 obtained HTS reads from spiked to naturally contaminated samples (Table 3).
402 Despite this observation, bioaccumulation experiments with fragmented norovirus
403 RNA and clinical samples established that the intact virus was preferentially
404 bioaccumulated over fragments of viral RNA and could survive up to two weeks (61).
405 In a previous trial, norovirus remained infectious for up to 61 days in groundwater at
406 room temperature. It persisted for up to 3 years based on RNase+ RT-qPCR assays
407 (62), though recent publications utilising the Human Intestinal Enteroid (HIE) models
408 have indicated a much shorter persistence of viable norovirus (63).
409
410 Furthermore, it has been well documented that noroviruses can be harboured within
411 biofilms, resulting in increased persistence (64) and binding to histo blood group
412 antigens (HBGA)-like molecules on enteric bacteria, increasing persistence and
413 enhancing viral pathogenesis (65, 66). As the target regions for RT-qPCR of
414 norovirus are < 100 bp, it is not surprising to observe less than a perfect agreement
415 between the HTS reads for 340/344 bp amplicons from a semi-nested PCR and gc/g
416 as per RT-qPCR amplicons. Therefore, it is challenging to define the probability that

417 norovirus viral RNA detected by RT-qPCR in shellfish is an intact and/or infectious
418 virus (67, 68).
419
420 While this study builds on previous work (5, 8, 67) and enhances the capacity for
421 surveillance and outbreak response on a national level, there are limitations. Much of
422 the work presented was performed with spiked samples, which are not necessarily
423 representative of naturally contaminated shellfish due to the quality and
424 concentration of the RNA. Unfortunately, RNA quality is difficult to assess in
425 molluscs due to a hidden break in the 28S (69), making it challenging to obtain a RIN
426 value. Therefore, we could not compare samples based on their RNA quality.
427 Additionally, we could not represent the full genetic diversity of noroviruses due to
428 limited access to clinical samples. Moreover, PCR-based sequencing will always be
429 biased due to the choice of primers.
430
431 We hypothesise that updated primer sets would permit the detection of additional
432 genotypes, particularly for norovirus GII.17, GII.3 and GI.3 (4, 21, 28, 70). While a
433 confusion matrix was used to assess method performance, an inter-laboratory ring
434 trial would provide a more realistic measure of method performance. Finally, clinical
435 genotyping of norovirus relies on the RdRp and VP1 of norovirus (23, 71, 72).
436 Ideally, the RdRp and VP1 should be amplified and sequenced in one amplicon, yet
437 Illumina limitations concerning read length do not permit this. The application of
438 Oxford Nanopore Technology or PacBio sequencing platforms would enable the
439 sequencing of longer amplicons and merits investigation.
440

441 This study provides a fit-for-purpose protocol for the genotypic characterisation of
442 norovirus in shellfish. We determined that Reverse Transcription and DNA
443 polymerase enzyme choice, technical triplicates and an optimised RNA extraction
444 procedure impact the quality and accuracy of HTS of norovirus amplicons. Wet-lab
445 methodology optimisation is pivotal in moving the field from *ad-hoc* sequencing to
446 accredited methods. The results provided here have wide-ranging implications for
447 HTS study design. Establishing standardised and well-described HTS methods, from
448 the wet lab to the bioinformatic analysis, is vital for building consensus in outbreak
449 investigations across shared jurisdictions. The methods we present here can be
450 applied for widespread surveillance of norovirus in complex samples such as
451 shellfish or wastewater to expand our understanding of norovirus diversity.

452

Methods

Samples

To assess the performance metrics, a series of three different experiments were performed. An overview of the sequencing libraries is provided in Table 8.

First, a proof-of-concept library was prepared and sequenced using SuperScript II and a selection of different DNA polymerases in both clinical (Table 1) and spiked samples (Table 9). A total of six stool samples were used as positive controls, while twelve matrix-specific mock communities were prepared.

Spiked and naturally contaminated samples were prepared in triplicate for a comprehensive RT and DNA polymerase enzyme comparison in the second experiment. The spiked sample was obtained from the proficiency testing scheme operated by the European Reference Laboratory for foodborne viruses (MIC200561). MIC200561 contained approximately 10000 copies of GI, and 1000 copies of GII (GI.3, GII.6, GII.7), while MIC180026 was a sample from a harvesting site collected in January 2018. It contained approximately 1000 gc/g GI and 4500 gc/g GII.

In the final experiment, three naturally contaminated oysters harvested in 2015 and 2016 were subject to an optimised protocol (RNA extraction to RT-PCR) to demonstrate the application of the method in the target samples, see Table 6.

Preparation of Oyster and Faecal Samples for Norovirus Analysis

In line with ISO 15216-1:2017, oysters were tested for the presence of norovirus GI and GII (73). In brief, oysters were cleaned before shucking and dissecting 10 oysters per sample. The dissected digestive tissue (DT) was diced and combined was a sterile razor blade. Samples were lysed with 2 ml Proteinase K (100 g ml^{-1}), followed by incubation and shaking at 37 °C for 60 minutes at 150 rpm. Samples underwent an additional incubation period of 15 minutes at 60 °C. Supernatants were retained for RNA extraction following centrifugation at 3000×g for 5 min.

For each stool sample, 0.5 ml PBS (Oxoid, UK) was added to a 2 ml tube containing between 2 g faecal material (neat) and vortexed vigorously. Then, 100 µl of the resuspended faecal material (neat) was transferred into a fresh tube containing 900 µl of PBS (10^{-1}) and serial dilutions were prepared up to 10^{-5}.

Viral RNA extraction

NucliSENS® magnetic extraction reagents (bioMérieux) and the NucliSENS® EasyMag® extraction platform were used to extract RNA from 500 µl of DT supernatants. This was then eluted into 100 µl of elution buffer. RNA extracts were kept at − 80 °C until the RT-qPCR or semi-nested PCR analysis was carried out. A single negative extraction control (water) was performed.

Determination of the Norovirus Concentration Using One-Step RT-qPCR

For samples where quantification of the norovirus RNA is provided, RT-qPCR was performed per ISO 15216-1:2017 (73). RT-qPCR analysis was performed using the Applied Biosystems AB7500 instrument (Applied Biosystems, Foster City, CA) and the RNA Ultrasense one-step RT-qPCR system (Invitrogen). The following were combined on a 96-well optical reaction plate to prepare the reaction mixture: 5 µl of RNA and 20 µl of the reaction mix containing 500 nM forward primer, 900 nM reverse primer, 250 nM sequence-specific probe, 1 × ROX reference dye and 1.25 µl of enzyme mix. Norovirus GI was detected using previously described primers QNIF4 (74), NV1LCR (75) and the TM9 probe (76), while QNIF2 (77), COG2R (78) and QNIFS probe (77) were used to detect norovirus GII. The internal process control mengovirus was detected using Mengo110, Mengo209 and Mengo147 probe (79). The plate was incubated at 55 °C for 60 min, 95 °C for 5 min, and then 45 cycles of PCR were performed, with 1 cycle consisting of 95 °C for 15 s, 60 °C for 1 min, and 65 °C for 1 min. All samples were analysed for norovirus GI and GII in duplicate. All control materials used in the RT-qPCR assays were prepared as previously described (80).

Preparation of matrix-specific mock communities

A panel of norovirus matrix-specific mock communities were generated using the positive control material (Table 1). Based on the genome copies (gc) per µl of each genotype, the weight of the norovirus-positive faecal sample to be added to the negative digestive tissue for the desired ratio was calculated and spiked into the homogenised norovirus-negative oyster digestive tissue. The total norovirus concentration in each mock community ranged

from 597 gc/g to 14292 gc/g of NoV GI or GII RNA, see Table 9.

cDNA generation and semi-nested PCR

cDNA was generated using either SuperScript II, SuperScript IV or LunaScript RT as per the manufacturer's protocols. Three DNA polymerases were evaluated for performance on the semi-nested PCR; AmpliTaq Gold, Kapa HiFi and Kapa Robust. For AmpliTaq Gold, the first round of nested PCR was prepared as follows, 5 µl cDNA was added to a 45 µl reaction mixture with a final concentration of 10 mM Tris-HCl (pH 8.3), 50 mM KCl, 20 µM of dNTPs, 2 µM of each primer (see Table 10), 2.5mM of MgCl2 and 2.5 U of AmpliTaq® DNA Polymerase (Applied Biosystems, USA). For the second round of PCR, the first round PCR product (5 µl) was added to 45 µl of a reaction mixture containing 10 mM Tris-HCl (pH 8.3), 50 mM KCl, 20 µM of dNTPs, 0.4 µM of each primer, 2.5 mM of MgCl2 and 2.5 U of AmpliTaq® DNA Polymerase.

For KAPA HiFi HotStart ReadyMix kit (Kapa Biosystems), the first round of PCR was prepared as follows: 5 µl cDNA with a final concentration of 10 µM of primers, 12.5 µl of KAPA HiFi HotStart ReadyMix and 2.5 µl of molecular grade biology water in a 25 µl reaction volume. For the second round of PCR, the first round PCR product (2.5 µl) was added to 22.5 µl of a reaction mixture containing a final concentration of 10 µM for primers, 12.5 µl of KAPA HiFi HotStart ReadyMix and 5 µl of molecular grade biology water. For KAPA2G Robust HotStart ReadyMix (Kapa Biosystems), the first round PCR was performed as follows: 5 µl cDNA with a final concentration of 10 µM of primers, 12.5 µl of KAPA2G Robust HotStart ReadyMix and 2.5 µl of molecular grade biology water. For the second round of PCR, the first round PCR

product (1 µl) was added to 24 µl of a reaction mixture containing a final concentration of 10 µM for primers, 12.5 µl of KAPA2G Robust HotStart ReadyMix and 6.5 µl of molecular grade biology water. PCR conditions are described in Table 11.

PCR individual or triplicates were performed during the first round of semi-nested PCR, using priming sites as shown in Figure 3. The primers for Sanger sequencing and HTS (see NGS primers) are provided in Table 10. Second-round PCR products were visualised on a 1x TAE 2% agarose gel containing 5 µl of Ethidium Bromide for clinical and spiked shellfish samples. The Agilent High Sensitivity DNA Kit for naturally contaminated shellfish was used to visualise second-round PCR products for Bioanalyzer 2100 (Agilent Technologies).

Cloning for Sanger sequencing

PCR amplicons were gel extracted using the QIAquick gel extraction kit and ligated into pGEM-T Easy plasmid (Promega). Vectors containing the PCR products were then cloned into chemically competent *E. coli*. Diluted and undiluted cells were plated on Luria Broth (LB) agar (Sigma, UK) containing XGal (20mg/ml), IPTG (100mM/ml) and Ampicillin (100mg/ml). Approximately ten to fifty colonies per sample were picked and purified using the QIAprep spin miniprep kit. PCR then confirmed the presence of the target DNA with M13 forward -20 (TGTAAAACGACGGCCAGT) and M13 reverse -27 primers (CAGGAAACAGCTATGAC) with Kapa Robust as per the manufacturer's instructions. Sanger sequencing was used to obtain the nucleic acid sequences of cloned fragments.

MiSeq library preparation and sequencing

Illumina sequencing adapters were incorporated into the second round PCR primers; see Table 10 for the sequences of the primers. PCR products were purified using Ampure XP beads (Beckmann Coulter) (0.8x bead:pool ratio) with elution of PCR products in 25 µl following the first bead clean-up. Cleaned-up PCR products were then indexed with the Nextera XT index kit (Illumina) following a modified 16S rRNA protocol from Illumina for use with the Nextera XT kit. Final indexed products (0.8x bead:pool ratio) were pooled to an equimolar concentration of 0.5-0.8nM. The Agilent High Sensitivity DNA Kit for Bioanalyzer 2100 (Agilent Technologies) was used to confirm amplicon presence, size and adapter-dimer removal. The cleaned pool was sequenced on an Illumina MiSeq sequencing platform with a 600-cycle V3 kit. All sequencing was performed at the Teagasc Sequencing Facility, per standard Illumina protocols.

Optimised RNA extraction to semi-nested PCR method

In order to improve the RNA yield from naturally contaminated shellfish, variations with regard to sample extract volume were included. RNA was extracted from 1000 µl of proteinase K extract and eluted into a smaller volume (30 µl). All samples were extracted in duplicate. LunaScript and AmpliTaq Gold provided the highest-quality HTS reads with minimum errors. RT with LunaScript was performed in triplicate to provide sufficient cDNA for semi-nested PCR of norovirus GI and GII targets in triplicate. cDNA was pooled and stored at -20°C. The first round of semi-nested PCR was prepared as follows, 10 µl cDNA per technical triplicate was added to a 45 µl reaction mixture with a final concentration of 10 mM Tris-HCl (pH 8.3), 50 mM KCl,

20 µM of dNTPs, 2 µM of each primer (see Table 10), 2.5mM of MgCl2 and 2.5 U of AmpliTaq® DNA Polymerase (Applied Biosystems, USA). The first round PCR product (5 µl) was subsequently added to 45 µl of a reaction mixture containing 10 mM TrisHCl (pH 8.3), 50 mM KCl, 20 µM of dNTPs, 0.4 µM of each primer, 2.5 mM of MgCl2 and 2.5 U of AmpliTaq® DNA Polymerase. The Agilent, High Sensitivity DNA Kit for Bioanalyzer 2100 (Agilent Technologies), was used to visualise second-round PCR products. Following library preparation, an additional Ampure bead clean-up step (0.7x bead:pool ratio) was performed to remove adapter dimers and 1 µl of the cleaned pool was visualised using the Agilent High Sensitivity DNA Kit for Bioanalyzer 2100 (Agilent Technologies) to confirm adapter-dimer removal.

Bioinformatic analysis

The pipeline utilised is based on the results from a previous study, which benchmarked pipelines and classifiers for norovirus amplicon analysis (81). Adapters and primers were trimmed using cutadapt (v 2.6) with an -e 0.1 and a minimum length of 100 bp. Reads were quality filtered in VSEARCH (v2.4.2) with a minimum length of 100 bp and a maximum length of 400 bp, a minimum overlap of 50 bp, a maximum of 20% mismatches in the alignment and a maximum expected error threshold of 1. Chimera removal was performed using UCHIME within VSEARCH (v2.4.2) using *de novo* and reference-based chimera removal, with 99% clustering prior to chimera detection. The database for chimera-based removal was generated as follows; all available norovirus sequences greater than 1000 bp were fetched from GenBank using rentrez (v1.2.3). VP1 sequences were created using the second-round primers outlined in Table 10 in seqkit (v1.4), and sequences were clustered to 85% identity using CD-HIT (v4.7). Clustering of the sequences following chimera

614 removal was performed at 99% identity, with a minimum of 1 read per sample
615 required for a true sequence. OTUs representing less than 1% of reads per sample
616 were removed. OTUs were classified using the NoroNet typing tool from RIVM.

617

Statistical analysis

All analysis was performed using R statistics (v 4.2.1) in R Studio. Kruskal-Wallis tests were performed in base R, while the post hoc test for Kruskal-Wallis was conducted using the Dunn test in the R package rstatix (v 0.7.0) (82). Factor Analysis of Mixed Data (FAMD) was performed using R package factoextra (v 1.7.0) (83) and factoMineR (v2.6.0) (84). DNA polymerase and RT enzyme were included as the factors of interest, alongside the numeric variable of interest such as mean Phred score or mean expected errors. Kendall correlation tests were performed using R statistics and interpreted based on previously reported ranks (34).

Distance matrices were conducted using the R package vegan (v 2.6.2). All distance measures were conducted using 999 permutations (Jaccard). Analysis of variance using distance matrices (ADONIS2) was also performed using the vegan package in R with Bonferroni p-value correction. Post Hoc tests for ANOSIM/ADONIS2 were performed using the R package RVAideMemoir (v 0.9-81-2).

A confusion matrix was generated using the yardstick package (v 1.0.9) in R from tidymodels (85). Data was coded in a binary fashion, encoding 1 for agreement between expected and observed data and zero for disagreement. Classifiers and databases were compared based on the sensitivity or true positive rate (TPR), false positive rate (FPR) or 1-specificity, F1 score and balanced accuracy (average of sensitivity and specificity). Sensitivity refers to the probability of obtaining a positive test for a true positive, and false positivity rate refers to the probability of obtaining a false positive test for a true negative or, in this case misclassification or missed classification. F1 score takes the harmonic mean of the sensitivity and specificity,

while balanced accuracy takes the mean of the sensitivity and specificity. Jaccard distance measures (R package vegan v 2.6.4) were used to assess true and false matches, between expected and observed data.

For UniFrac analysis, files were imported into QIIME2/2021.2. Sequences were aligned using the MAFFT plugin and masked. For UniFrac analysis, rooted trees were generated using rooted fastree and distances computed with all tips.

Custom BLAST databases were created based on the expected data for each library 1 and 2. Observed output for each sample was blasted against the custom database, requiring 99% similarity at 75% coverage of the amplicon. Multiple hits for an observed sequence to a reference sequence in the BLAST DB were filtered. The observed OTU with the highest bit-score and lowest e-value per sample/library was selected for the comparison if multiple hits were obtained.

Data availability

Sequence data generated during the current study have been deposited in the European Nucleotide Archive under accession number PRJEB58629.

Data Availability

The scripts used for the processing of bioinformatic data are available at https://github.com/ahfitzpa/Norovirus_HTS_amplicon. The dataset generated and analysed during the current study is available in the ENA repository under accession number PRJEB58629.

Author Contributions

AHF, AR and SK designed the experiments. AR prepared the spiked samples, from RNA extraction to sample characterisation using Sanger sequencing. AHF performed RT-PCRs, library preparation and bioinformatic analysis and wrote the manuscript. FC sequenced all libraries at the Teagasc Next Generation DNA Sequencing Facility. SK, HO'S and PC reviewed the final draft. All authors contributed to the article and approved the submitted version.

Funding

This work was funded by the Cullen Scholarship Programme, which is carried out with the support of the Marine Institute and funded under the Marine Research Programme by the Irish Government (Funding call: CF/18/01/01).

Conflict of Interest

The authors declare that the research was conducted without any commercial or financial relationships that could be construed as a potential conflict of interest.

Acknowledgements

Figures 1–2, and Supplementary Figure 1 were created with BioRender.com. The authors would like to thank Leon Devilly and James Fahy (Shellfish Microbiology team, Marine Institute) for their assistance with sample preparation for sequencing, Elaine Lawton and Teagasc Next Generation DNA Sequencing Facility for supporting this work.

References

1. Rajko-Nenow P, Waters A, Keaveney S, Flannery J, Tuite G, Coughlan S, O'Flaherty V, Dore W. 2013. Norovirus Genotypes Present in Oysters and in Effluent from a Wastewater Treatment Plant during the Seasonal Peak of Infections in Ireland in 2010. Applied and Environmental Microbiology 79:2578–2587.

2. Rajko-Nenow P, Keaveney S, Flannery J, O'Flaherty V, Doré W. 2012. Characterisation of norovirus contamination in an Irish shellfishery using real-time RT-qPCR and sequencing analysis. International Journal of Food Microbiology 160:105–112.

3. Rajko-Nenow P, Keaveney S, Flannery J, McIntyre A, Dore W. 2013. Norovirus genotypes implicated in two oyster-related illness outbreaks in Ireland. Epidemiology and Infection 142:2096–2104.

4. Suffredini E, Iaconelli M, Equestre M, Valdazo-González B, Ciccaglione AR, Marcantonio C, Della Libera S, Bignami F, La Rosa G. 2017. Genetic Diversity Among Genogroup II Noroviruses and Progressive Emergence of GII.17 in Wastewaters in Italy (2011-2016) Revealed by Next-Generation and Sanger Sequencing. Food Environ Virol https://doi.org/10.1007/s12560-017-9328-y.

5. Imamura S, Kanezashi H, Goshima T, Haruna M, Okada T, Inagaki N, Uema M, Noda M, Akimoto K. 2017. Next-Generation Sequencing Analysis of the Diversity of Human Noroviruses in Japanese Oysters. Foodborne Pathogens and Disease 14:465–471.

6. Raymond P, Paul S, Perron A, Bellehumeur C, Larocque É, Charest H. 2022. Detection and Sequencing of Multiple Human Norovirus Genotypes from Imported Frozen Raspberries Linked to Outbreaks in the Province of Quebec, Canada, in 2017. Food Environ Virol https://doi.org/10.1007/s12560-021-09507-8.

712 7. Buytaers FE, Verhaegen B, Gand M, D'aes J, Vanneste K, Roosens NHC, Marchal K,
713 Denayer S, De Keersmaecker SCJ. 2022. Metagenomics to Detect and Characterize
714 Viruses in Food Samples at Genome Level? Lessons Learnt from a Norovirus Study.
715 21. Foods 11:3348.

716 8. Strubbia S, Schaeffer J, Besnard A, Wacrenier C, Le Mennec C, Garry P, Desdouits M,
717 Le Guyader FS. 2020. Metagenomic to evaluate norovirus genomic diversity in oysters:
718 Impact on hexamer selection and targeted capture-based enrichment. International
719 Journal of Food Microbiology 323:108588.

720 9. Strubbia S, Phan MVT, Schaeffer J, Koopmans M, Cotten M, Le Guyader FS. 2019.
721 Characterization of Norovirus and Other Human Enteric Viruses in Sewage and Stool
722 Samples Through Next-Generation Sequencing. Food Environ Virol
723 https://doi.org/10.1007/s12560-019-09402-3.

724 10. Imamura S, Haruna M, Goshima T, Kanezashi H, Okada T, Akimoto K. 2016.
725 Application of Next-Generation Sequencing to Evaluate the Profile of Noroviruses in
726 Pre- and Post-Depurated Oysters. Foodborne Pathogens and Disease 13:559–565.

727 11. Hjelmsø MH, Mollerup S, Jensen RH, Pietroni C, Lukjancenko O, Schultz AC,
728 Aarestrup FM, Hansen AJ. 2019. Metagenomic analysis of viruses in toilet waste from
729 long distance flights—A new procedure for global infectious disease surveillance. PLOS
730 ONE 14:e0210368.

731 12. Hellmér M. 2018. Viral Metagenomics to Assess the Microbial Quality of Reused
732 Wastewater. Technical University of Denmark, Kgs. Lyngby, Denmark.

733 13. Fumian TM, Fioretti JM, Lun JH, dos Santos IAL, White PA, Miagostovich MP. 2019.
734 Detection of norovirus epidemic genotypes in raw sewage using next generation
735 sequencing. Environment International 123:282–291.

14. Bartsch C, Höper D, Mäde D, Johne R. 2018. Analysis of frozen strawberries involved in a large norovirus gastroenteritis outbreak using next generation sequencing and digital PCR. Food Microbiology 76:390–395.

15. Boonchan M, Motomura K, Inoue K, Ode H, Chu PY, Lin M, Iwatani Y, Ruchusatsawat K, Guntapong R, Tacharoenmuang R, Chantaroj S, Tatsumi M, Takeda N, Sangkitporn S. 2017. Distribution of norovirus genotypes and subtypes in river water by ultra-deep sequencing-based analysis. Letters in Applied Microbiology 65:98–104.

16. Joanna Ollivier, James Lowther, Marion Desdouits, Julien Schaeffer, Candice Wacrenier, Bas B. Oude Munnink, Alban Besnard, Frederico Mota Batista, Tina Stapleton, Anna Charlotte Schultz, Frank Aarestrup, Marion Koopmans, Miranda de Graaf, Soizick Le Guyader. 2022. Application of Next Generation Sequencing on Norovirus-contaminated oyster samples. EFSA supporting publications https://doi.org/10.2903/sp.efsa.2022.en-7348.

17. Ollivier J, Lowther J, Desdouits M, Schaeffer J, Wacrenier C, Oude Munnink BB, Besnard A, Mota Batista F, Stapleton T, Schultz AC, Aarestrup F, Koopmans M, de Graaf M, Le Guyader S. 2022. Application of Next Generation Sequencing on Norovirus-contaminated oyster samples. EFSA Supporting Publications 19:7348E.

18. Bernard H, Werber D, Höhle M. 2014. Estimating the under-reporting of norovirus illness in Germany utilizing enhanced awareness of diarrhoea during a large outbreak of Shiga toxin-producing E. coli O104:H4 in 2011 – a time series analysis. BMC Infectious Diseases 14:116.

19. Hofmann FM, Olawumi E, Michaelis M, Hofmann F, Stößel U. 2020. Challenges in Infection Epidemiology: On the Underreporting of Norovirus Gastroenteritis Cases in Germany. 1. International Journal of Environmental Research and Public Health 17:314.

761 20. Hallowell BD, Parashar UD, Hall AJ. 2019. Epidemiologic challenges in norovirus
762 vaccine development. Human Vaccines & Immunotherapeutics 15:1279–1283.

763 21. Bonura F, Urone N, Bonura C, Mangiaracina L, Filizzolo C, Sciortino G, Sanfilippo GL,
764 Martella V, Giammanco GM, De Grazia S. 2021. Recombinant GII.P16 genotype
765 challenges RT-PCR-based typing in region A of norovirus genome. Journal of Infection
766 https://doi.org/10.1016/j.jinf.2021.04.015.

767 22. Green SJ, Venkatramanan R, Naqib A. 2015. Deconstructing the Polymerase Chain
768 Reaction: Understanding and Correcting Bias Associated with Primer Degeneracies
769 and Primer-Template Mismatches. PLOS ONE 10:e0128122.

770 23. Chhabra P, de Graaf M, Parra GI, Chan MC-W, Green K, Martella V, Wang Q, White
771 PA, Katayama K, Vennema H, Koopmans MPG, Vinjé J. 2019. Updated classification
772 of norovirus genogroups and genotypes. Journal of General Virology
773 https://doi.org/10.1099/jgv.0.001318.

774 24. Vinjé J, Hamidjaja RA, Sobsey MD. 2004. Development and application of a capsid
775 VP1 (region D) based reverse transcription PCR assay for genotyping of genogroup I
776 and II noroviruses. Journal of Virological Methods 116:109–117.

777 25. Vinjé J. 2015. Advances in Laboratory Methods for Detection and Typing of Norovirus.
778 Journal of Clinical Microbiology 53:373–381.

779 26. Parra GI, Squires RB, Karangwa CK, Johnson JA, Lepore CJ, Sosnovtsev SV, Green
780 KY. 2017. Static and Evolving Norovirus Genotypes: Implications for Epidemiology and
781 Immunity. PLOS Pathogens 13:e1006136.

782 27. Wang S, Xu X, Wei C, Li S, Zhao J, Zheng Y, Liu X, Zeng X, Yuan W, Peng S. 2022.
783 Molecular evolutionary characteristics of SARS-CoV-2 emerging in the United States.
784 Journal of Medical Virology 94:310–317.

785 28. Dong L, Jia T, Yu Y, Wang Y. 2022. Updating a New Semi-nested PCR Primer Pair for
786 the Specific Detection of GII Norovirus in Oysters. Food Environ Virol
787 https://doi.org/10.1007/s12560-022-09511-6.

788 29. Vinjé J. 2015. Advances in Laboratory Methods for Detection and Typing of Norovirus.
789 Journal of Clinical Microbiology 53:373–381.

790 30. Zucha D, Androvic P, Kubista M, Valihrach L. 2020. Performance Comparison of
791 Reverse Transcriptases for Single-Cell Studies. Clin Chem 66:217–228.

792 31. Cholet F, Ijaz UZ, Smith CJ. 2020. Reverse transcriptase enzyme and priming strategy
793 affect quantification and diversity of environmental transcripts. Environmental
794 Microbiology n/a.

795 32. Sze MA, Schloss PD. 2019. The Impact of DNA Polymerase and Number of Rounds of
796 Amplification in PCR on 16S rRNA Gene Sequence Data. mSphere 4:e00163-19.

797 33. Dabney J, Meyer M. 2012. Length and GC-biases during sequencing library
798 amplification: A comparison of various polymerase-buffer systems with ancient and
799 modern DNA sequencing libraries. BioTechniques 52:87–94.

800 34. Landis JR, Koch GG. 1977. The Measurement of Observer Agreement for Categorical
801 Data. Biometrics 33:159–174.

802 35. Bustin SA. 2000. Absolute quantification of mRNA using real-time reverse transcription
803 polymerase chain reaction assays. Journal of Molecular Endocrinology 25:169–193.

804 36. Šťovíček A, Cohen-Chalamish S, Gillor O. 2019. The effect of reverse transcription
805 enzymes and conditions on high throughput amplicon sequencing of the 16S rRNA.
806 PeerJ 7:e7608.

807 37. Stangegaard M, Høgh Dufva I, Dufva M. 2006. Reverse transcription using random
808 pentadecamer primers increases yield and quality of resulting cDNA. BioTechniques
809 40:649–657.

810 38. Kebelmann-Betzing C, Seeger K, Dragon S, Schmitt G, Möricke A, Schild TA, Henze
811 G, Beyermann B. 1998. Advantages of a New Taq DNA Polymerase in Multiplex PCR
812 and Time-Release PCR. BioTechniques 24:154–158.

813 39. Nilsson M, Grånemo J, Buś MM, Havsjö M, Allen M. 2016. Comparison of DNA
814 polymerases for improved forensic analysis of challenging samples. Forensic Science
815 International: Genetics 24:55–59.

816 40. Maunula L, Kaupke A, Vasickova P, Söderberg K, Kozyra I, Lazic S, van der Poel
817 WHM, Bouwknegt M, Rutjes S, Willems KA, Moloney R, D'Agostino M, de Roda
818 Husman AM, von Bonsdorff C-H, Rzeżutka A, Pavlik I, Petrovic T, Cook N. 2013.
819 Tracing enteric viruses in the European berry fruit supply chain. International Journal of
820 Food Microbiology 167:177–185.

821 41. Smits SL, Schapendonk CME, Leeuwen M van, Kuiken T, Bodewes R, Raj VS,
822 Haagmans BL, Neves CG das, Tryland M, Osterhaus ADME. 2013. Identification and
823 Characterization of Two Novel Viruses in Ocular Infections in Reindeer. PLOS ONE
824 8:e69711.

825 42. Herm R, Tummeleht L, Jürison M, Vilem A, Viltrop A. 2020. Trace amounts of African
826 swine fever virus DNA detected in insects collected from an infected pig farm in
827 Estonia. Veterinary Medicine and Science 6:100–104.

828 43. Damaso N, Ashe EC, Meiklejohn KA, Kavlick MF, Robertson JM. 2021. Comparison of
829 polymerases used for amplification of mitochondrial DNA from challenging hairs and
830 hairs of various treatments. Forensic Science International: Genetics 52:102484.

831 44. Reifenberger GC, Thomas BA, Rhodes DVL. 2022. Comparison of DNA Extraction and
832 Amplification Techniques for Use with Engorged Hard-Bodied Ticks. 6. Microorganisms
833 10:1254.

834 45. Witte AK, Sickha R, Mester P, Fister S, Schoder D, Rossmanith P. 2018. Essential role
835 of polymerases for assay performance – Impact of polymerase replacement in a well-
836 established assay. Biomolecular Detection and Quantification 16:12–20.

837 46. Levesque-Sergerie J-P, Duquette M, Thibault C, Delbecchi L, Bissonnette N. 2007.
838 Detection limits of several commercial reverse transcriptase enzymes: impact on the
839 low- and high-abundance transcript levels assessed by quantitative RT-PCR. BMC
840 Molecular Biology 8:93.

841 47. Nichols RV, Vollmers C, Newsom LA, Wang Y, Heintzman PD, Leighton M, Green RE,
842 Shapiro B. 2018. Minimizing polymerase biases in metabarcoding. Molecular Ecology
843 Resources 18:927–939.

844 48. Nayak MK, Balasubramanian G, Sahoo GC, Bhattacharya R, Vinjé J, Kobayashi N,
845 Chawla Sarkar M, Bhattacharya M, Krishnan T. 2008. Detection of a novel
846 intergenogroup recombinant Norovirus from Kolkata, India. Virology 377:117–123.

847 49. Rohayem J, Münch J, Rethwilm A. 2005. Evidence of Recombination in the Norovirus
848 Capsid Gene. Journal of Virology 79:4977–4990.

849 50. Aird D, Ross MG, Chen W-S, Danielsson M, Fennell T, Russ C, Jaffe DB, Nusbaum C,
850 Gnirke A. 2011. Analyzing and minimizing PCR amplification bias in Illumina
851 sequencing libraries. Genome Biology 12:R18.

852 51. Tyson JR, James P, Stoddart D, Sparks N, Wickenhagen A, Hall G, Choi JH, Lapointe
853 H, Kamelian K, Smith AD, Prystajecky N, Goodfellow I, Wilson SJ, Harrigan R, Snutch
854 TP, Loman NJ, Quick J. 2020. Improvements to the ARTIC multiplex PCR method for

855 SARS-CoV-2 genome sequencing using nanopore. bioRxiv
856 https://doi.org/10.1101/2020.09.04.283077.

857 52. Wang C, Sensale S, Pan Z, Senapati S, Chang H-C. 2021. Slowing down DNA
858 translocation through solid-state nanopores by edge-field leakage. 1. Nat Commun
859 12:140.

860 53. ISO. 2017. ISO 21872-1:2017 - Microbiology of the food chain -- Horizontal method for
861 the determination of Vibrio spp. -- Part 1: Detection of potentially enteropathogenic
862 Vibrio parahaemolyticus, Vibrio cholerae and Vibrio vulnificus.
863 https://www.iso.org/standard/74112.html. Retrieved 9 April 2019.

864 54. Leifels M, Shoults D, Wiedemeyer A, Ashbolt NJ, Sozzi E, Hagemeier A, Jurzik L.
865 2019. Capsid Integrity qPCR—An Azo-Dye Based and Culture-Independent Approach
866 to Estimate Adenovirus Infectivity after Disinfection and in the Aquatic Environment.
867 Water 11:1196.

868 55. Leifels M, Cheng D, Sozzi E, Shoults DC, Wuertz S, Mongkolsuk S, Sirikanchana K.
869 2021. Capsid integrity quantitative PCR to determine virus infectivity in environmental
870 and food applications – A systematic review. Water Research X 11:100080.

871 56. Manuel CS, Moore MD, Jaykus L-A. 2018. Predicting human norovirus infectivity -
872 Recent advances and continued challenges. Food Microbiology 76:337–345.

873 57. Walker DI, Cross LJ, Stapleton TA, Jenkins CL, Lees DN, Lowther JA. 2019.
874 Assessment of the Applicability of Capsid-Integrity Assays for Detecting Infectious
875 Norovirus Inactivated by Heat or UV Irradiation. Food Environ Virol
876 https://doi.org/10.1007/s12560-019-09390-4.

877 58. Knight A, Haines J, Stals A, Li D, Uyttendaele M, Knight A, Jaykus L-A. 2016. A
878 systematic review of human norovirus survival reveals a greater persistence of human

879 norovirus RT-qPCR signals compared to those of cultivable surrogate viruses.
880 International Journal of Food Microbiology 216:40–49.

881 59. Lee CS. 2018. Genomic integrity of human norovirus and F-RNA bacteriophage as
882 detected by RT-qPCR and its relationship to infectivity before and after UV-treatment.
883 Thesis. NUI Galway.

884 60. Weng S, Dunkin N, Schwab KJ, McQuarrie J, Bell K, Jacangelo JG. 2018. Infectivity
885 reduction efficacy of UV irradiation and peracetic acid-UV combined treatment on MS2
886 bacteriophage and murine norovirus in secondary wastewater effluent. Journal of
887 Environmental Management 221:1–9.

888 61. Dancer D, Rangdale RE, Lowther JA, Lees DN. 2010. Human norovirus RNA persists
889 in seawater under simulated winter conditions but does not bioaccumulate efficiently in
890 Pacific Oysters (Crassostrea gigas). Journal of Food Protection 73:2123–2127.

891 62. Seitz SR, Leon JS, Schwab KJ, Lyon GM, Dowd M, McDaniels M, Abdulhafid G,
892 Fernandez ML, Lindesmith LC, Baric RS, Moe CL. 2011. Norovirus Infectivity in
893 Humans and Persistence in Water. Applied and Environmental Microbiology 77:6884–
894 6888.

895 63. Shaffer M, Huynh K, Costantini V, Bibby K, Vinjé J. 2022. Viable Norovirus Persistence
896 in Water Microcosms. Environ Sci Technol Lett 9:851–855.

897 64. Skraber S, Ogorzaly L, Helmi K, Maul A, Hoffman L, Cauchie HM, Gantzer C. 2009.
898 Occurrence and Persistence of enteroviruses, noroviruses and F-specific RNA phages
899 in natural wastewater biofilms. Water Research.

900 65. Almand EA, Moore MD, Outlaw J, Jaykus L-A. 2017. Human norovirus binding to select
901 bacteria representative of the human gut microbiota. PLoS One; San Francisco
902 12:e0173124.

903 66. Amarasiri M, Sano D. 2019. Specific Interactions between Human Norovirus and
904 Environmental Matrices: Effects on the Virus Ecology. Viruses 11:224.

905 67. Desdouits M, Polo D, Mennec CL, Strubbia S, Zeng X-L, Ettayebi K, Atmar RL, Estes
906 MK, Guyader FSL. Use of Human Intestinal Enteroids to Evaluate Persistence of
907 Infectious Human Norovirus in Seawater - Volume 28, Number 7—July 2022 -
908 Emerging Infectious Diseases journal - CDC https://doi.org/10.3201/eid2807.220219.

909 68. Hunt K. 2019. A Risk Assessment of Norovirus in Irish Produced Raw Oysters. PhD
910 thesis. UCD, University Colege Dublin.

911 69. Adema CM. 2021. Sticky problems: extraction of nucleic acids from molluscs.
912 Philosophical Transactions of the Royal Society B: Biological Sciences 376:20200162.

913 70. Salazar E, Miraba M, Villaquiran J, Aguirre B, Suarez K, Cevallos J. 2022.
914 Development of enhanced primer sets for detection of norovirus and hepatitis A in food
915 samples from Guayaquil (Ecuador) by reverse transcriptase-heminested PCR
916 https://doi.org/10.21203/rs.3.rs-1658924/v1.

917 71. Chhabra P, Browne H, Huynh T, Diez-Valcarce M, Barclay L, Kosek MN, Ahmed T,
918 Lopez MR, Pan C-Y, Vinjé J. 2020. Single-step RT-PCR assay for dual genotyping of
919 GI and GII norovirus strains. Journal of Clinical Virology 104689.

920 72. de Graaf M, Villabruna N, Koopmans MP. 2017. Capturing norovirus transmission.
921 Current Opinion in Virology 22:64–70.

922 73. ISO 15216. 2017. Microbiology of the food chain — Horizontal method for
923 determination of hepatitis A virus and norovirus using real-time RT-PCR — Part 1:
924 Method for quantification.

925 74. da Silva AK, Le Saux JC, Parnaudeau S, Pommepuy M, Elimelech M, Le Guyader FS.
926 2007. Evaluation of removal of noroviruses during wastewater treatment, using real-

927 time reverse transcription-PCR: different behaviours of genogroups I and II. Applied
928 and Environmental Microbiology 73:7891–97.

929 75. Svraka S, Duizer E, Vennema H, de Bruin E, van de Veer B, Dorresteijn B, Koopmans
930 M. 2007. Etiological role of viruses in outbreaks of acute gastroenteritis in The
931 Netherlands from 1994 through 2005. Journal of Clinical Microbiology 45:1389–1394.

932 76. Hoehne M, Schreier E. 2006. Detection of Norovirus genogroup I and II by multiplex
933 real-time RT- PCR using a 3'-minor groove binder-DNA probe. BMC Infectious
934 Diseases 6.

935 77. Loisy F, Atmar RL, Guillon P, Le Cann P, Pommepuy M, Le Guyager FS. 2005. Real-
936 time RT-PCR for norovirus screening in shellfish. Journal of Virological Methods 123:1–
937 7.

938 78. Kageyama T, Kojima S, Shinohara M, Uchida K, Fukushi S, Hoshino FB, Takeda N,
939 Katayama K. 2003. Broadly reactive and highly sensitive assay for Norwalk-like viruses
940 based on real-time quantitative reverse transcription-PCR. Journal of Clinical
941 Microbiology 41:1548–1557.

942 79. Pintó RM, Costafreda MI, Bosch A. 2009. Risk Assessment in Shellfish-Borne
943 Outbreaks of Hepatitis A. Applied and Environmental Microbiology 75:7350–7355.

944 80. Flannery J, Keaveney S, Rajko-Nenow P, O'Flaherty V, Doré WJ. 2012. Concentration
945 of Norovirus during Wastewater Treatment and Its Impact on Oyster Contamination.
946 Applied and Enviromental Microbiology 78:3400–6.

947 81. Fitzpatrick AH, Rupnik A, O'Shea H, Crispie F, Keaveney S, Cotter PD. 2022.
948 Benchmarking Bioinformatic Tools for Amplicon-Based Sequencing of Norovirus.
949 Applied and Environmental Microbiology https://doi.org/10.1128/aem.01522-22.

82. Kassambara A. 2021. rstatix: Pipe-Friendly Framework for Basic Statistical Tests (0.7.0).

83. Kassambara A, Mundt F. 2019. factoextra: Extract and visualize the results of multivariate data analyses.

84. Husson F, Josse J, Le S, Mazet J. 2022. FactoMineR: Multivariate Exploratory Data Analysis and Data Mining (2.6).

85. Kuhn M, Wickham H. 2020. Tidymodels: a collection of packages for modeling and machine learning using tidyverse principles.

Figure legends and tables

Table 1: Sanger sequencing results for clinical samples used in the proof-of-concept library and spiking experiments. Norovirus (NoV) detection is reported in genome copies per microlitre (gc/µL) for GI and GII. Genotypic characterisation of Sanger sequences from each sample was performed using NoroNet.

Sample ID	NoV GI gc/µL	NoV GII gc/µL	Genotype NoroNet
FM011		1.03^{04}	GII.3
FM012		1.67^{03}	GII.2
FM018		1.18^{05}	GII.4 Sydney 2012
FM022	5.47^{03}		GI.4
FM023		3.23^{06}	GII.4
FM026	3.26^{02}		GI.9

968 **Table 2:** Genotypes detected using amplicon HTS across all sample types prepared
969 with the selected RT and DNA polymerase enzymes. Genotypic characterisation of
970 HTS Operational Taxonomic Units (OTUs) was performed using NoroNet.

Enzyme combination	Genotype NoroNet
SuperScript II / AmpliTaq Gold	GI.3, GI.4, GI.7, GI.9, GII.2, GII.3, GII.4, GII.4 New Orleans 2009, GII.4 Sydney 2012, GII.6
SuperScript II / Kapa HiFi	GI.3, GI.4, GI.7, GI.9, GII.2, GII.3, GII.4, GII.4 New Orleans 2009, GII.4 Sydney 2012, GII.6
SuperScript II / Kapa Robust	GI.3, GI.4, GI.7, GI.9, GII.2, GII.3, GII.4, GII.4 New Orleans 2009, GII.4 Sydney 2012, GII.6
SuperScript IV / AmpliTaq Gold	GI.3, GI.7, GII.6, GII.7
SuperScript IV / Kapa HiFi	GI.3, GI.7, GII.6, GII.7
SuperScript IV / Kapa Robust	GI.1, GI.3, GI.7, GII.2, GII.6, GII.7
LunaScript / AmpliTaq Gold	GI.1, GI.3, GI.7, GI.9, GII.13, GII.14, GII.4 Sydney 2012, GII.6, GII.7
LunaScript / Kapa HiFi	GI.1, GI.3, GI.7, GII.6
LunaScript / Kapa Robust	GI.3, GI.7, GII.4 Sydney 2012, GII.6

971

972

973 **Table. 3** Kendall correlation between gc/g of norovirus detected by RT-qPCR
974 prior to semi-nested PCR or ng/ul of DNA following semi-nested PCR and library
975 preparation and reads after QC with HTS reads following quality control in
976 spiked shellfish samples

Matrix	RT and DNA polymerase enzyme	Number of genotypes	Kendall correlation between gc/g of norovirus detected by RT-qPCR (pre-PCR) and reads after QC	Kendall correlation between ng/ul of DNA after library preparation and reads after QC	N
Spiked oyster	SuperScript II AmpliTaq Gold	single	0.667, p-value 0.33	1.000, p-value 0.08	4
Spiked oyster	SuperScript II Kapa Robust	single	0.000, p-value 1.00	0.000, p-value 1.00	4
Spiked oyster	SuperScript II AmpliTaq Gold	multiple	-0.247, p-value 0.24	0.871, p-value < 0.05	6
Spiked oyster	SuperScript II Kapa HiFi	multiple	0.871, p-value 0.51	-0.567 p-value < 0.05	6
Spiked oyster	SuperScript II Kapa Robust	multiple	-0.141, p-value < 0.05	0.591 p-value < 0.05	6

977

978

979 **Table 4.** Performance of RT and DNA polymerase enzymes to genotype level

980 classification as per a confusion matrix

RT and DNA polymerase	Matrix	Technical replicates	accuracy	sensitivity	specificity	precision	recall	f-measure
LunaScript AmpliTaq Gold	Spiked oyster	Triplicates	1.00	1.00	1.00	1.00	1.00	1.00
LunaScript Kapa HiFi	Spiked oyster	Triplicates	1.00	1.00	1.00	1.00	1.00	1.00
LunaScript Kapa Robust	Spiked oyster	Triplicates	1.00	1.00	1.00	1.00	1.00	1.00
SuperScript II AmpliTaq Gold	Spiked oyster	Individual	1.00	1.00	1.00	1.00	1.00	1.00
	Spiked oyster	Triplicate	0.86	0.83	1.00	1.00	0.83	0.91
SuperScript II Kapa HiFi	Spiked oyster	Individual	0.96	0.95	1.00	1.00	0.95	0.98
	Spiked oyster	Triplicate	1.00	1.00	1.00	1.00	1.00	1.00
SuperScript II Kapa Robust	Spiked oyster	Individual	1.00	1.00	1.00	1.00	1.00	1.00
	Spiked oyster	Triplicate	0.86	0.83	1.00	1.00	0.83	0.91
SuperScript IV AmpliTaq Gold	Spiked oyster	Triplicate	1.00	1.00	1.00	1.00	1.00	1.00
SuperScript IV Kapa HiFi	Spiked oyster	Triplicate	1.00	1.00	1.00	1.00	1.00	1.00
SuperScript IV Kapa Robust	Spiked oyster	Triplicate	1.00	1.00	1.00	1.00	1.00	1.00

981

Table 5. Performance of RT and DNA polymerase enzymes in pooled GI and GII amplicons to genotype level classification as per a confusion matrix

RT and DNA polymerase enzyme	Matrix	accuracy	sensitivity	specificity	precision	recall	f-measure
LunaScript Kapa HiFi	Spiked oyster	1.00	1.00	1.00	1.00	1.00	1.00
SuperScript II Kapa HiFi	Spiked oyster	1.00	1.00	1.00	1.00	1.00	1.00
SuperScript IV Kapa HiFi	Spiked oyster	1.00	1.00	1.00	1.00	1.00	1.00
LunaScript Kapa Robust	Spiked oyster	1.00	1.00	1.00	1.00	1.00	1.00
SuperScript IV AmpliTaq Gold	Spiked oyster	0.86	0.83	1.00	1.00	0.83	0.91
SuperScript II Kapa Robust	Spiked oyster	0.86	0.83	1.00	1.00	0.83	0.91
SuperScript IV Kapa Robust	Spiked oyster	0.86	0.83	1.00	1.00	0.83	0.91
LunaScript AmpliTaq Gold	Spiked oyster	0.71	0.67	1.00	1.00	0.67	0.80
SuperScript II AmpliTaq Gold	Spiked oyster	0.71	0.67	1.00	1.00	0.67	0.80

Table 6: Naturally contaminated samples sequenced using Sanger and HTS

Sample ID	NoV GII genome copies/g
MIC15592	543
MIC16714	2556
MIC16945	102

Table. 7 Norovirus genotypes detected using both Sanger sequencing and HTS amplicon sequencing

Sample	Sanger with cloning of isolates	Amplicon HTS MiSeq
MIC15592	GII.14	GII.14, GII.6
MIC16714	GII.6, GII.4 Sydney 2012, GII.13	GII.4 Sydney 2012, GII.13, GII.6, GII.7
MIC16945	GII.6	GII.6

996 **Table 8:** Overview of sequencing experiments

Experiment	**sample matrix**	**Technical replicates**	**No of biological samples**	**Total PCR products**	**Genotypes Expected**
Proof of concept	clinical & spiked shellfish	Individual	18 (6 clinical & 12 spiked shellfish samples)	59	GI.4, GI.9, GII.3, GII.2, GII.4 Sydney 2012, GII.4
RT and DNA polymerase comparison	spiked & naturally contaminated shellfish	Triplicate	2	98	GI.3, GI.7, GII.6
Application in naturally contaminated shellfish	naturally contaminated shellfish	Triplicate	3	10	unknown

997

998 **Table 9:** Spiked samples using in experiment one

Genotype	GII 2000-5000 gc/µl			GI 2000-5000 gc/µl	GII 1000 gc/µl	single 1000 gc/µl						GI 1000 gc/µl
	1	2	3	4	5	6	7	8	9	10	11	12
GI.4				Present		Present						Present
GI.9				Present			Present					Present
GII.3	Present	Present	Present		Present			Present				
GII.2	Present	Present	Present		Present				Present			
GII.4 Sydney	Present	Present	Present		Present					Present		
GII.4	Present	Present	Present		Present						Present	
gc/g qPCR ABI	13424	14292	13705	4012	2868	1233	2402	700	785	1209	597	4279

999

1000

1001

1002 **Table 10:** Primers used for amplification of VP1 capsid gene in Sanger and

1003 Illumina sequencing

Genogroup	Primer	Sequence (5′ → 3′)	semi-nested PCR	Polarity	Study
GI	COG1F	CGYTGGATGCGNTTYCATGA	1st	+	(78)
	G1SKR	CCAACCCARCCATTRTACA	1st and 2nd	–	(81)
	G1SKF	CTGCCCGAATTYGTAAATGA	2nd	–	(81)
	G1SKF NGS	GTCTCGTGGGCTCGGAGATGTGTATAAGAGACAG CCAACCCARCCATTRTACA	2nd NGS	+	
	G1SKR NGS	TCGTCGGCAGCGTCAGATGTGTATAAGAGACAGCT GCCCGAATTYGTAAATGA	2nd NGS	–	
GII	COG2F	CARGARBCNATGTTYAGRTGGATGAG	1st	+	(78)
	GIISKR	CCRCCNGCATRHCCRTTRTACAT	1st and 2nd	–	(81)
	GIISKF	CNTGGGAGGGCGATCGCAA	2nd	+	(81)
	GIISKF NGS	TCGTCGGCAGCGTCAGATGTGTATAAGAGACAGC NTGGGAGGGCGATCGCAA	2nd NGS	+	
	GIISKR NGS	GTCTCGTGGGCTCGGAGATGTGTATAAGAGACAG CCRCCNGCATRHCCRTTRTACAT	2nd NGS	–	

1004

1005

1006

1007 **Table 11:** PCR conditions for the norovirus capsid region

	Kapa Robust	**Kapa Robust**	**AmpliTaq Gold**	**Kapa HiFi**	**AmpliTaq Gold**	**AmpliTaqGold**
	1st round:	2nd round:	1st round:	2nd round:	1st round No heated lid	2nd round
	95°C 3 min;	95°C 3 min;	95°C 5 min;	95°C 3 min;	95°C 5 min;	95°C 5 min;
PCR Cycling Conditions	*40x:* 95°C 15 sec 50°C 15 sec 72°C 15 sec	*30x:* 95°C 15 sec 55°C 15 sec 72°C 15 sec	*40x:* 95°C 1 min 50°C 1 min 72°C 2 min	*25x:* 95°C 30 sec 55°C 30 sec 72°C 30 sec	*40x:* 95°C 1 min 50°C 1 min 72°C 2 min	*40x:* 95°C 1 min 50°C 1 min 72°C 2 min
	72°C 1 min	72°C 1 min	72°C 15 min	72°C 1 min	72°C 15 min	72°C 15 min

1008

1009

1010

Figure 1. Violin plots with (A) an internal boxplot of the mean Phred score (Q) obtained in spiked shellfish and naturally contaminated oysters. RT and DNA polymerase combinations are ordered from highest mean Phred score to lowest (left to right). **(B) Violin plots** with internal boxplot of the mean expected errors (EE). RT and DNA polymerase combinations are ordered from the highest mean expected error score to the lowest (left to right).

Figure 2.A Factor analysis with mixed data (FAMD) biplot demonstrates the variance-maximising distribution patterns of the total Mean Phred scores in the map space and their clustering patterns based on DNA polymerase and RT enzyme. **B. FAMD biplot** for DNA polymerase demonstrates the variance-maximising distribution patterns of the total Mean Expected Errors in the map space and their clustering patterns based on DNA Polymerase and RT enzyme.

Figure 3: Regions of norovirus genome used for genotypic characterisation and detection by RT-qPCR.

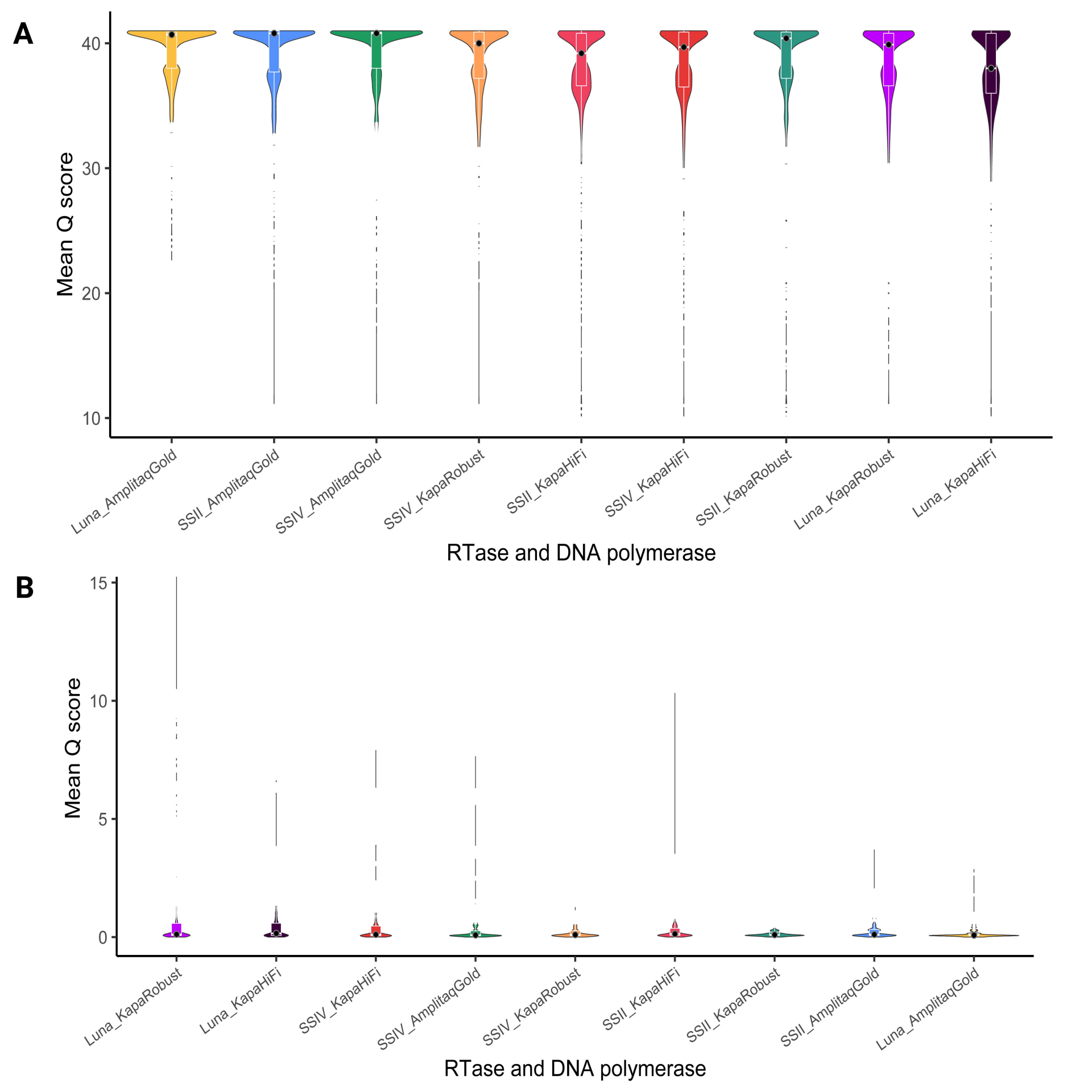
A
Mean Q score
40
30
20
10
Luna_AmplitaqGold
SSII_AmplitaqGold
SSIV_AmplitaqGold
SSIV_KapaRobust
SSII_KapaHiFi
SSIV_KapaHiFi
SSII_KapaRobust
Luna_KapaRobust
Luna_KapaHiFi
RTase and DNA polymerase
B
Mean Q score
15
10
5
0
Luna_KapaRobust
Luna_KapaHiFi
SSIV_KapaHiFi
SSIV_AmplitaqGold
SSIV_KapaRobust
SSII_KapaHiFi
SSII_KapaRobust
SSII_AmplitaqGold
Luna_AmplitaqGold
RTase and DNA polymerase

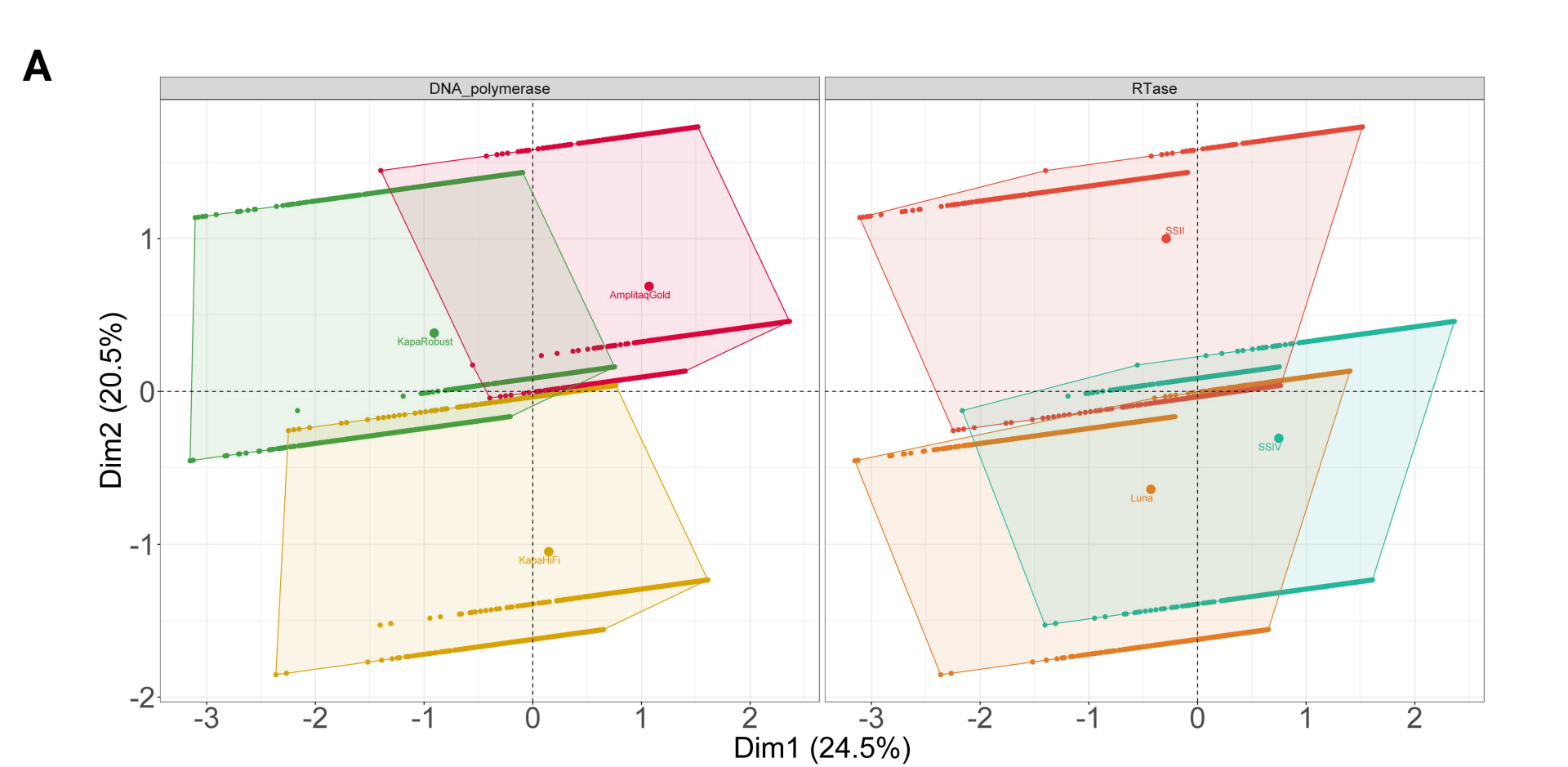
A
DNA_polymerase
RTase
AmplitaqGold
KapaRobust
KapaHiFi
SSII
SSIV
Luna
Dim2 (20.5%)
Dim1 (24.5%)

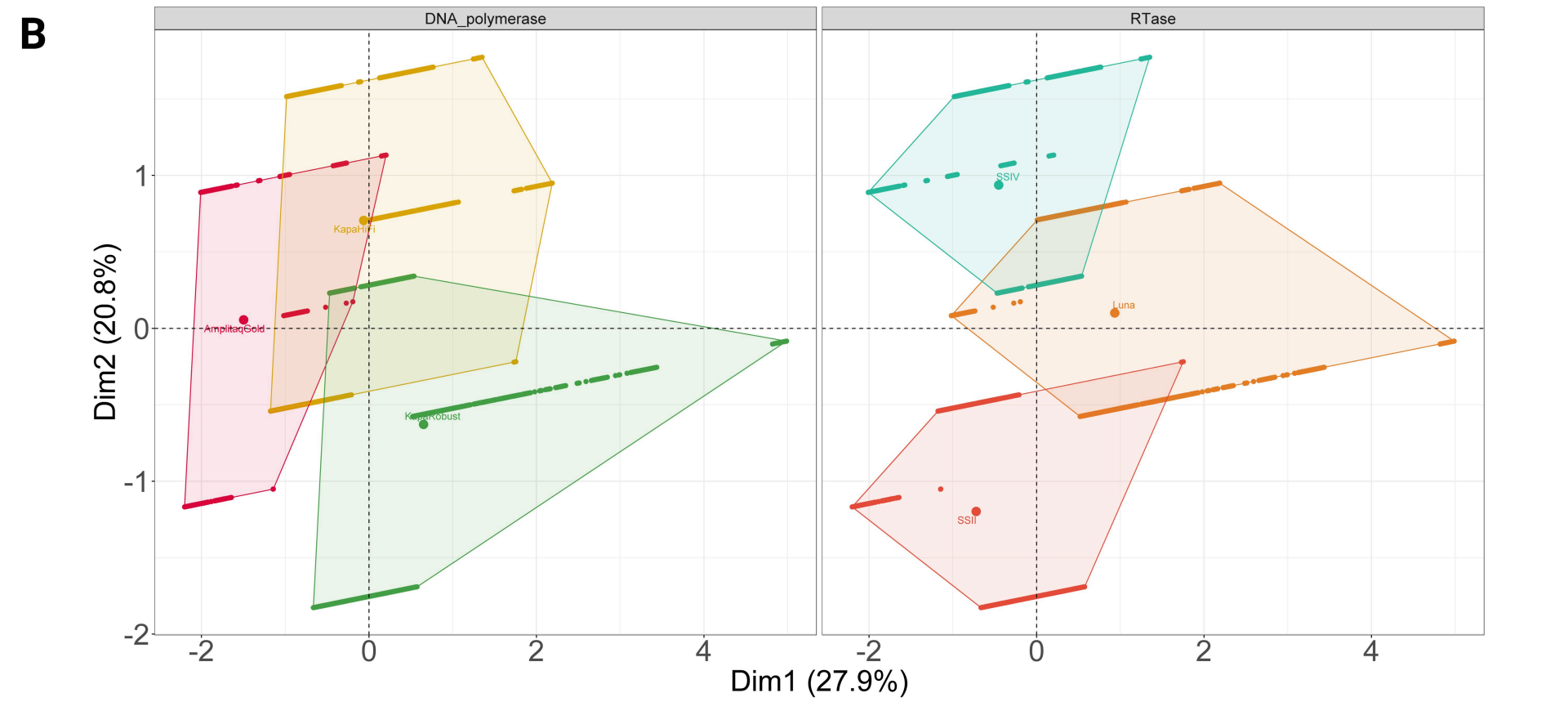
B
DNA_polymerase
RTase
KapaHiFi
AmplitaqGold
KapaRobust
SSIV
Luna
SSII
Dim2 (20.8%)
Dim1 (27.9%)

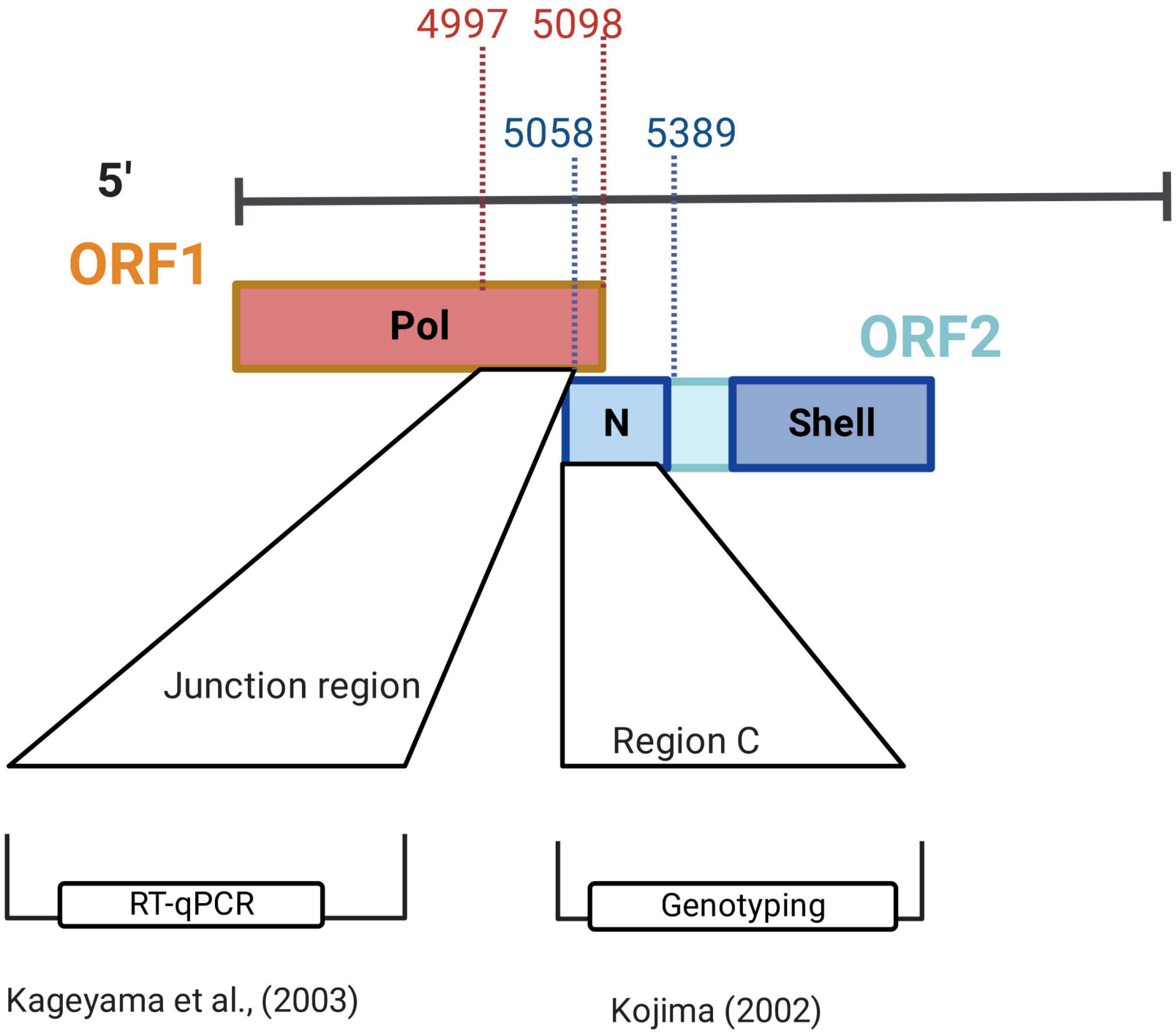
4997
5098
5058
5389
5'
ORF1
Pol
ORF2
N
Shell
Junction region
Region C
RT-qPCR
Genotyping
Kageyama et al., (2003)
Kojima (2002)

Benchmarking of norovirus amplicon HTS

A method for genotypic characterisation of norovirus VPI in shellfish